Anales de Mecánica de la Fractura

TEXTO DE LAS COMUNICACIONES PRESENTADAS EN EL

1st VIRTUAL IBERIAN CONFERENCE ON STRUCTURAL INTEGRITY

Número 37

25, 26 y 27 de marzo de 2020

Anales de Mecánica de la Fractura

Texto de las comunicaciones presentadas en el

1st Virtual Iberian Conference on Structural Integrity

25, 26 y 27 de marzo de 2020

Editado por la Secretaría del Grupo Español de Fractura

I.S.S.N.: 0213-3725
Fecha publicación: diciembre 2020

EDITORIAL

El volumen 37 de los Anales de Mecánica de la Fractura incluye las comunicaciones presentadas en la 1st Virtual Iberian Conference on Structural Integrity. Esta primera edición virtual sustituye a la 5th Iberian Conference on Structural Integrity que, en principio, se iba a celebrar en Coimbra el 25, 26 y 27 de marzo del 2020, y que tuvo que ser suspendido debido a la situación mundial de la pandemia generada por el COVID-19. En esta ocasión, la organización del congreso, promovido por la Sociedad Portuguesa de Integridad Estructural y el Grupo Español de Fractura – Sociedad Española de Integridad Estructural, ha recaído en la Universidad de Coimbra y en el Politécnico de Coimbra.

Los congresos ibéricos o hispano-portugueses se han celebrado en cuatro ocasiones: Braga (1987), Mérida (1993), Luso (1996) y Porto (2010). Y han sido un foro de encuentro de investigadores y profesionales interesados en la integridad de materiales y estructuras, contituyendo el marco ideal para mostrar avances e intercambiar ideas entre los investigadores de España y Portugal.

Deseamos agradecer el trabajo y el esfuerzo de todos los autores que han hecho posible la edición de este volumen asociado a la primera conferencia virtual con un total de 57 trabajos.

También expresamos nuestro agradecimiento a los miembros del Comité Científico, quienes han participado activamente en la organización de la conferencia.
En diciembre de 2020

El Comité Organizador

EDITORIAL

Volume 37 of the Annals of Fracture Mechanics includes the communications presented at the I Iberian Virtual Congress on Structural Integrity. This first virtual edition has been launched since the 5th Iberian Conference on Structural Integrity which, in principle, would be held in Coimbra on March 25, 26 and 27, 2020 had to be postponed to 2021 due to the global situation of the pandemic generated by COVID-19. On this occasion, the organization of the congress promoted by the Portuguese Society of Structural Integrity and the Spanish Group of Fracture - Spanish Society of Structural Integrity has fallen to the University of Coimbra and the Polytechnic of Coimbra.

Iberian or Spanish-Portuguese congresses have been held on four occasions: Braga (1987), Mérida (1993), Luso (1996) and Porto (2010). And they have been a meeting forum for researchers and professionals interested in the integrity of materials and structures, being the opportunity to show progress and exchange ideas between researchers from Spain and Portugal.

We wish to thank the work and effort of all the authors who have made possible the edition of this volume associated with the first virtual conference with a total of 57 papers.

We also wish to thank the members of the Scientific Committee, who have actively participated in the organization.

December 2020

The Organizing Committee

Junta Directiva de la Sociedad Española de Integridad Estructural – Grupo Español de Fractura (SEIE-GEF)

Presidente:	Francisco Gálvez Díaz-Rubio (Universidad Politécnica de Madrid)
Vicepresidente 1º:	Jesús Manuel Alegre Calderón (Universidad de Burgos)
Vicepresidente 2º:	Eugenio Giner Maravilla (Universidad de Valencia)
Vicepresidente 3º:	Cristina Rodríguez González (Universidad de Oviedo)
Vicepresidente 4º:	Carlos Navarro Pintado (Universidad de Sevilla)
Vicepresidente 5º:	Orlando Santana Pérez (Universidad Politécnica de Cataluña)
Secretaria:	Alicia Salazar López (Universidad Rey Juan Carlos)
Tesorero:	Luis Távara Mendoza (Universidad de Sevilla)

Organizadores del 1st Virtual Iberian Conference on Structural Integrity

Presidentes del Comité Organizador

Luís Filipe Borrego

José Martins Ferreira

Comité Organizador

José Domingos Costa

Pedro Moreira

Virgínia Infante

Fernando Ventura Antunes

Ricardo Branco

Comité Científico

Abílio de Jesus
(Universidade do Porto)

Alfredo da Silva Ribeiro
(Universidade de Trás-os-Montes e Alto Douro)

Andrés Valiente Cancho
(Universidad Politécnica de Madrid)

António Mário Henriques Pereira
(Escola Superior de Tecnologia e Gestão de Leiria)

Alfonso Fernández Canteli
(Universidad de Oviedo)

Alicia Salazar López
(Universidad Rey Juan Carlos)

António Augusto Fernandes
(Universidade do Porto)

Antonio Martín Meizoso
(Universidad de Navarra, CEIT)

Armando Ramalho
(Politécnico de Castelo Branco)
Carlos Capela
(Escola Superior de Tecnologia e Gestão de Leiria)
Carmen Baudín
(Instituto de Cerámica y vidrio, CSIC)
Emilio García Pañeda
(Imperial College London)
Fernando Ventura Antunes
(Universidade de Coimbra)
Francisco Gálvez Díaz-Rubio
(Universidad Politécnica de Madrid)
Idoia Urrutibeascoa
(Universidad de Mondragón)
Jaime Planas Roselló
(Universidad Politécnica de Madrid)
Jesús Manuel Alegre Calderón (Universidad de Burgos)
José Alberto Álvarez Laso
Universidad de Cantabria)
José Cardoso Xavier
(Universidade Nova de Lisboa)
José Fernández Sáez
(Universidad Carlos III de Madrid)

Luís F. G. Reis
(Instituto Superior Técnico)

Luís Roseiro
(Instituto Superior de Engenharia de Coimbra)
Mª Lluisa Maspoch
Universidad Politécnica de Cataluña)
Manuel Moreira de Freitas
(Instituto Superior Técnico)
Paulo Nobre dos Reis
(Universidade da Beira Interior)

Paulo Tavares (INEGI)

Pedro Moreira (INEGI)

Belen Moreno
(Universidad de Málaga)

Carlos Navarro Pintado
(Universidad de Sevilla)

Cristina Rodríguez González
(Universidad de Oviedo)
Eugenio Giner Maravilla
(Universidad Politécnica de Valencia)
Filipe Samuel Silva
(Universidade do Minho)
Gonzalo Ruíz López
(Universidad de Castilla - La Mancha)
Jaime Domínguez Abascal
(Universidad de Sevilla)

Javier Belzunce (Universidad de Oviedo)

Jesús Toribio Quevedo
(Universidad de Salamanca)
José António Correia
(Universidade do Porto)
José Domingos Costa
(Universidade de Coimbra)
José Martins Ferreira
(Universidade de Coimbra)
Luís Filipe Borrego
(Instituto Superior de Engenharia de Coimbra)
Luis Távara Mendoza
(Universidad de Sevilla)
Manuel Fonte
(Escola Superior Náutica)
Orlando Santana Pérez
(Universidad Politécnica de Cataluña)
Paulo Tavares de Castro
(Universidade do Porto)
Pedro Bravo Díez
(Universidad de Burgos)
Ricardo Batista
(Instituto Politécnico de Setúbal)

Ricardo Branco
(Universidade de Coimbra)
Rui F. Martins
(Universidade Nova de Lisboa)
Virgínia Infante (Instituto Superior Técnico)

Ricardo Cláudio
(Instituto Politécnico de Setúbal)
Sergio Cicero González
(Universidad de Cantabria)

Patrocinadores

ÍNDICE

AN OCTREE-BASED ADAPTIVE MESH REFINEMENT FOR ADDITIVE MANUFACTURING

B.M. Marques[1*], D.M. Neto[1], M.C. Oliveira[1]

[1] University of Coimbra, CEMMPRE, Department of Mechanical Engineering,
Rua Luís Reis Santos, Pinhal de Marrocos, 3030-788 Coimbra, Portugal
[*] Contact person: bruno.marques@uc.pt

RESUMEN

Se ha prestado cada vez más atención a los procesos de fabricación aditiva (AM) debido a su capacidad para producir piezas complejas y personalizadas. Con el fin de evitar la lenta y costosa experimentación física de ensayo y error, se ha adoptado un modelado numérico para comprender los fenómenos involucrados en el proceso. Sin embargo, el costo de las simulaciones numéricas es muy alto debido a la naturaleza multifísica y multiescala. Con el fin de reducir el tiempo computacional del análisis de elementos finitos, se puede adoptar el refinamiento de malla adaptable (AMR), lo que permite reducir significativamente el número de elementos finitos sin pérdida de precisión. Este estudio presenta un nuevo algoritmo AMR basado en octree, desarrollado específicamente para la simulación AM, donde las mallas no conformes generadas están compuestas por elementos finitos hexaédricos lineales. Los criterios utilizados para el refinamiento/engrosamiento de cada zona se basan en la trayectoria del láser, particularmente la región alrededor del láser, que se caracteriza por grandes gradientes de temperatura. El algoritmo propuesto garantiza un equilibrio 2:1 entre los elementos vecinos y permite la deposición multicapa por la estrategia de activación de elementos, que divide el dominio en elementos finitos activos e inactivos. Los resultados muestran que el procedimiento propuesto permite la generación de mallas no conformes con un número total de elementos un 99% inferior a una malla conformante.

PALABRAS CLAVE: Fabricación aditiva, Elementos finitos, Refinamiento de malla adaptable, Malla octree

ABSTRACT

Increasing attention has been given to additive manufacturing (AM) processes due to their ability to produce complex and customized parts. In order to avoid the slow and expensive trial-and-error physical experimentation, numerical modelling has been adopted to understand the phenomena involved in the process. However, the cost of the numerical simulations is very high due to the multi-physics and multi-scale nature. In order to reduce the computational time of the finite element analysis, the adaptive mesh refinement (AMR) can be adopted, allowing to significantly reduce the number of finite elements without loss of accuracy. This study presents a new octree-based AMR algorithm, specifically developed for AM simulation, where the generated non-conforming meshes are composed by linear hexahedral finite elements. The criteria used for the refinement/coarsening of each zone is based on the laser path, particularly the region around the laser spot, which is characterized by large temperature gradients. The proposed algorithm guarantees a 2:1 balance between neighbouring elements and allows multi-layer deposition by element activation strategy, which divides the domain into active and inactive finite elements. The results show that the proposed procedure enables the generation of non-conformal meshes with a total number of elements 99% lower than a conformal mesh with similar minimum element size.

KEYWORDS: Additive manufacturing; Finite element simulation; Adaptive mesh refinement; Octree mesh

INTRODUCTION

In the last decade, additive manufacturing (AM) processes have received increasing attention to produce highly customized and complex components, particularly the powder bed fusion technology for metallic components [1]. Nevertheless, the unwanted residual stresses and distortions of the final component are unresolved issues associated with the AM process [2, 3]. Indeed, the part distortion yields low dimensional accuracy, while the presence of residual stresses can deteriorate the fatigue strength of the component [4]. Therefore, the optimization of the process parameters is vital for the AM success, which is very expensive and time consuming using exclusively trial-and-error experiments [5]. On the other hand, numerical simulation can provide a better understanding of the AM process, increases the predictability of the component properties and establishes optimization guidelines for the manufacturing process. However, the computational cost of numerical simulations can be very high due to the multi-physics and multi-scale nature of the AM

process. Indeed, the numerical modelling of AM processes requires a very high computational effort, particularly when combined with the need for the simulation of the entire thermo-mechanical history [6].

Both the accuracy of the numerical solution and the computational time are strongly dependent of the finite element mesh adopted in the numerical analysis. Regarding the generation of the finite element mesh, the meshes can be divided into two groups: conforming and non-conforming. Although most of the finite element analysis resort to conforming meshes, the numerical simulation of AM processes takes advantage of non-conforming meshes due to the high degree of flexibility for discretizing the region where a fine mesh is required [7]. The main drawback of non-conforming meshes is the presence of hanging nodes, which require a special treatment to enforce the continuity. The adoption of non-conforming structured meshes to refine the region of interest is called Adaptive Mesh Refinement (AMR), which is used to enrich the region around the laser with a much denser mesh. Besides, the AMR can be further divided into static AMR and dynamic AMR [8]. The static AMR uses the same finite element mesh during the entire simulation process, while the dynamic AMR updates the refined region accordingly to either the laser position or the state variables (temperature gradients). Since the powder bed fusion AM processes present extremely high-temperature gradients near the (moving) melt pool, the adoption of a dynamic AMR approach in the simulation process allows to reduce the computational time in comparison with the static AMR approach [9]. However, the dynamic AMR approach requires the update of the finite element mesh, which is a time-consuming task due to the generation/elimination of elements and remapping of the state variables between meshes.

Considering the use of non-conforming meshes, the mesh refinement is achieved by element split, i.e. the bisection procedure is applied to each parent element, which is replaced by eight (assuming a hexahedral element) children elements. On the other hand, the coarsening is obtained by recovering parent element from the corresponding children elements. Since a fast and easy access to the hierarchical information is required for computational efficiency, a tree data structure (called octree) is usually adopted, which establishes the hierarchical information between parent and children elements through the element level. The octree is analogous to a binary tree (maximum of two children per element) in one dimension and to a quadtree (maximum of four children per element) in two dimensions. The simple Cartesian structure and embedded hierarchy, make octree-based mesh adaptation, reconstruction and data access fairly fast and easy [10] which is ideal for dynamic AMR.

In this paper, an octree-based AMR algorithm is presented with additive manufacturing applications in mind. The algorithm uses an enrichment h-refinement procedure to produce corner balanced refinements for local portions of the mesh. Moreover, multi-layer deposition is integrated in the proposed algorithm, based on the element activation strategy [11].

ADAPTIVE MESH REFINEMENT ALGORITHM

An octree-based data structure [12] is used to store mesh-related information required for the mesh refinement/coarsening procedure. This provides easy and fast access to all finite element's information, allowing to achieve fast computational times for dynamic AMR. The root of the tree is the initial mesh, composed by hexahedral finite elements in the present study, which is also the coarser mesh used in the dynamic AMR procedure. The level 0 is assigned to this initial mesh, while the level of the children is one level higher than its parent [13]. Figure 1 (a) presents an example illustrating the relationship between the mesh domain and the corresponding octree-based hierarchical data structure. The initial mesh was composed by a single hexahedral finite element (level 0). Due to the bisection procedure, this element was replaced by eight children elements of level 1 (cyan). In order to generate a gradient in the mesh refinement, only a single child element of level 1 was replaced by the corresponding children elements of level 2 (orange). Finally, only a single child element of level 2 was replaced by the corresponding children elements of level 3 (red). The final mesh is composed by finite elements of three different sizes, corresponding to the level 1 up to level 3. This information is stored in an octree-based structure schematically presented in Figure 1 (b), where the empty squares represent the parent elements, which are disabled and replaced by their respective enabled children. This type of data structure is very efficient for storing the required information, allowing to develop efficient algorithms for mesh refinement/coarsening.

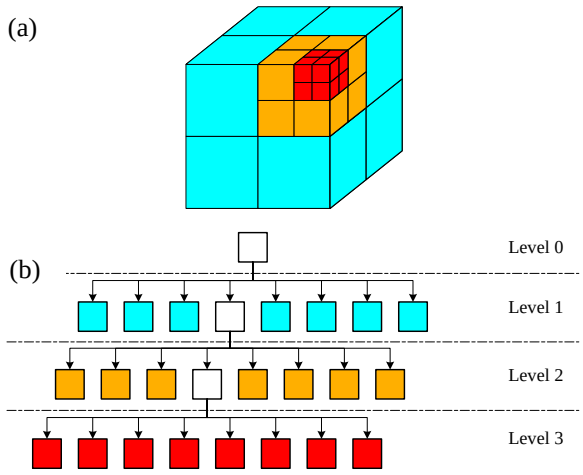

Figure 1. Three-dimensional adaptive mesh refinement: (a) generated cartesian mesh of the block; (b) corresponding octree-based hierarchical data structure.

2.1. Mesh refinement procedure

The proposed mesh refinement procedure takes into account the laser path, since this location requires a fine mesh to capture the severe temperature gradients. Moreover, the volume around the laser beam containing the fine mesh is defined taking into account the volumetric heat source adopted in the finite element model, which in this work was the double ellipsoidal heat source [14]. In order to avoid the presence of hanging nodes in this region of interest, the finite elements with maximum level of refinement (user defined) are contained within an amplified size of the volumetric heat source. The update of the finite element mesh in each time step of the simulation according to the current position of the laser is very time consuming, while the refinement of the entire laser path leads to excessive finite elements. Accordingly, the laser path is divided into a finite number of stages, which are refined sequentially through the movement of the amplified heat source volume. Each stage of the laser path covers the current and the forthcoming position of the laser beam.

Figure 2 presents the flowchart of the proposed mesh refinement procedure adopted in the AMR. The volume to be refined is defined by the movement of the amplified heat source volume over the initial mesh (level 0). The first step comprises a cycle over the finite elements of level 0 to identify which of them are contained (totally or partially) by this volume. Then, the elements identified as been contained by this volume are disabled and replaced by the corresponding children (eight for each parent), which are finite elements of level 1, to be used in the next cycle. This procedure is recursively repeated until the entire amplified heat source volume is discretized with finite element of the maximum level (defined by the user).

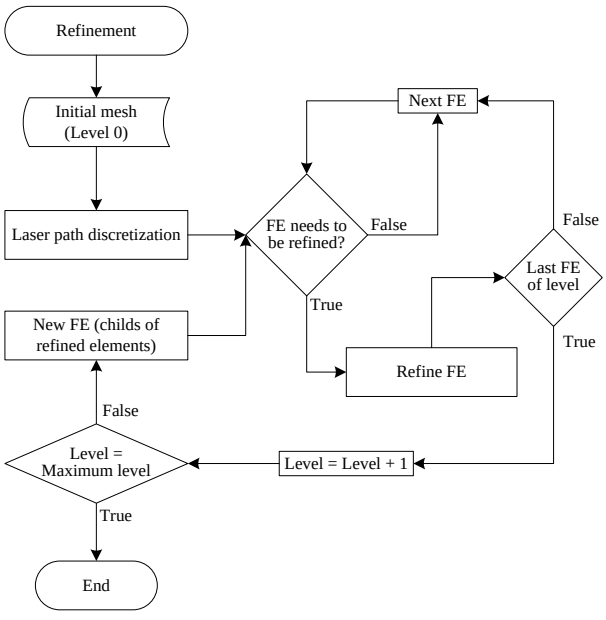

Figure 2. Flowchart of the mesh refinement procedure adopted in the AMR.

2.2. Mesh coarsening procedure

The main purpose of the mesh coarsening procedure is to recover the initial coarse mesh once the laser moves away. This allows to reduce the total number of finite elements present in the mesh and, consequently, the simulation time. Figure 3 presents the flowchart of the proposed mesh coarsening procedure adopted in the AMR. The first step comprises a cycle over the finite elements with the maximum level, which are selected for coarsening, i.e. the refinement level will decrease by enabling the parent elements and disabling their children. This procedure is performed recursively ($Level = Level - 1$) until level 0 is reached or the element size is restricted by the powder layer thickness. This way the developed algorithm guarantees that the element size (element level) is enough to describe appropriately the thickness of the powder layer.

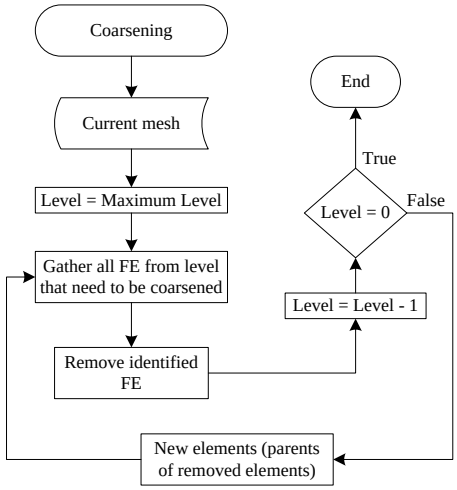

Figure 3. Flowchart of the mesh coarsening procedure adopted in the AMR.

2.3. Balancing rule across finite elements

In order to ensure that there is at most one hanging node on any edge or face, the 2:1 balance constraint is imposed to the octree-based hexahedral meshes. The balance refinement is a nonlocal and inherently iterative process [13]. The corner balanced refinement occurs when the difference in the level of all finite elements sharing the same node is at most one. In order to ensure this, the balancing rule is applied during the refinement and the coarsening procedures, previously described. In case of refinement, the balancing algorithm guarantees that all nodes of the selected element present a level with the shared elements at least equal to the level of the selected element. On the other hand, in the coarsening procedure, the balancing algorithm guarantees that all nodes of the selected element present a level with the shared elements at most equal to the level of the selected element. Figure 4 presents the flowchart of the proposed balancing procedure adopted in the AMR. If the refinement/coarsening of a finite element leads to

corner unbalance, the neighbour elements responsible by creating the unbalance are selected for refinement/coarsening. This process is applied recursively until the corner balance is achieved. However, due to the nature of the coarsening process, the coarsening of a given element might not be possible due to the surrounding elements. Therefore, the coarsening criterion is verified when applying the balancing rule across finite elements.

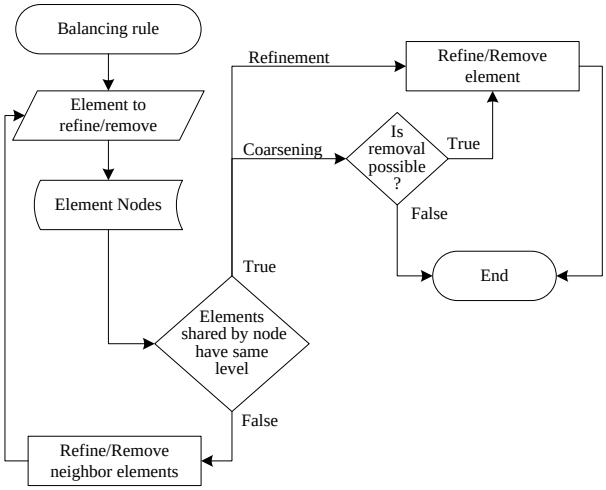

Figure 4. Flowchart of the balancing algorithm adopted in the AMR.

2.4. Powder layer deposition

Since the parts are built layer-by-layer in the AM processes, the modelling of the material deposition is required in the numerical simulation. Therefore, the proposed algorithm considers the multi-layer deposition. This is achieved by adopting the element activation strategy proposed by [11], which divides the domain into active and inactive finite elements. Finite elements above the top powder layer plane (ghost elements) are considered inactive, while finite elements below are considered active. The first step of the layer deposition algorithm is to determine the element level that yields a finite element size identical to the powder layer thickness, called layer level. Then, the mesh refinement procedure is applied until achieving a uniform mesh in the layer domain, i.e. the level of each element is the same as the layer level.

Figure 5 presents the flowchart of the proposed powder layer deposition procedure adopted in the AMR. The intersection of the upper surface of the powder layer with the initial mesh is performed in order to identify the set of parent finite elements (level 0), which are replaced by the corresponding children elements if not yet enabled. This process is repeated until all enabled elements intersected by the upper surface of the powder layer present the same level as the layer level.

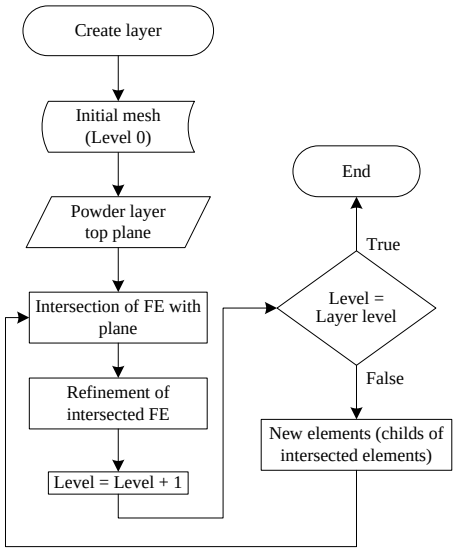

Figure 5. Flowchart of the powder layer deposition procedure adopted in the AMR.

NUMERICAL EXAMPLES

3.1. Adaptive mesh refinement in layer deposition

The geometry adopted in this example is a parallelepiped with 1.6 mm×1.6 mm×1.28 mm, divided into 2 regions: volume of the substrate (lower half part) and volume for powder deposition (upper half part). The initial mesh (level 0) is composed of 100 hexahedral finite elements, using 5 finite elements both in the length and in the width directions, while only 4 elements are defined in the height direction (see Figure 6 (a) for lateral view). The layer thickness considered is 0.040 mm, which corresponds to a finite element refinement of level 3. Since the upper surface of the first powder layer is located at $z = 0.680$ mm, the intersection of the initial mesh with this plane identifies all elements (level 0) next to the substrate, which are them replaced by their children elements. Moving to the next element level (level 1), all children elements previously stored are checked for intersection with the same plane, resulting once more, in all elements of level 1 next to the substrate, which are replaced by their children elements. This procedure is repeated until a uniform layer of elements of level 3 is created, corresponding to the powder layer thickness. Figure 6 (b) presents the lateral view of the mesh at the end of the first layer deposition process, highlighting the powder layer at orange. The same procedure applies to the deposition of the second and third layers, but the intersection is made against the $z = 0.720$ mm plane for the second layer, and against $z = 0.760$ mm plane for the third layer. Figure 6 (c) presents the lateral plane view of the mesh at the end of the second layer deposition process. Figure 6 (d) presents the lateral view of the mesh at the end of the third layer deposition process, where it is possible to visualize the merge of the two first layers (deposited over the substrate), allowing to reduce the total number of elements.

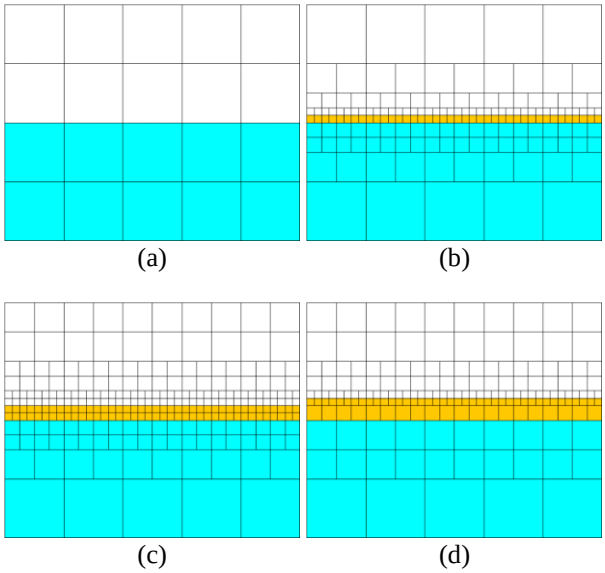

Figure 6. Example of layer deposition: (a) initial mesh covering the substrate (cyan) and the inactive elements (white); (b) substrate with the first powder layer (orange); (c) substrate with the two powder layers (orange); (d) substrate with the three powder layers (orange); first two layers are merged.

3.2. Adaptive mesh refinement in a single track

This example aims to highlight the ability of the proposed algorithm to perform the refinement and coarsening of the finite element mesh according to the laser path. Both the geometry and the initial mesh is the same used in the previous example. However, the inactive elements are hidden only for visualization reasons, as shown in Figure 7 (a). This example is composed of three distinct steps: (i) deposition of the first powder layer; (ii) adaptive refinement of a straight laser trajectory in four stages; (iii) deposition of the second powder layer. The procedure described in the previous example is used to perform the deposition of the first and second powder layers, leading to the mesh configuration presented in Figure 7 (b) and Figure 7 (g), respectively. Regarding the adaptative mesh refinement of the laser path, the total path length is divided into four stages with 40% of the total length, using an overlap of 20%. The mesh of the powder layer is refined in the region corresponding to the laser path (stage), using the coarsening procedure in the region behind the section, as shown in Figure 7 (c)-(f).

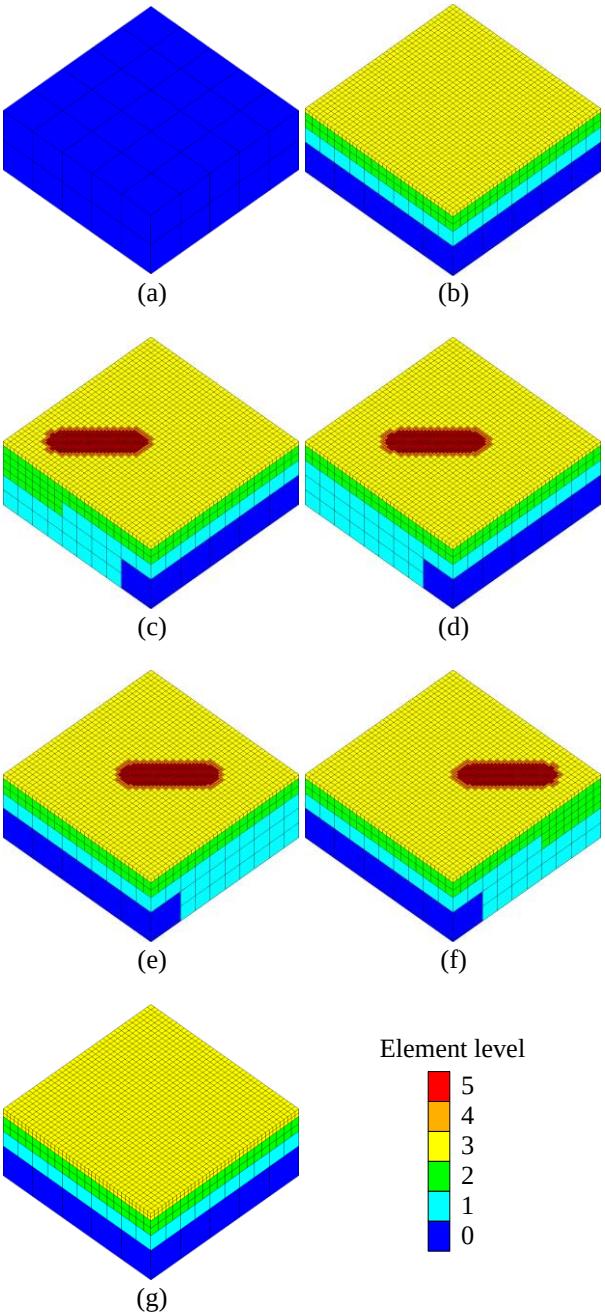

Figure 7. Example of mesh refinement in a single track: (a) substrate; (b) substrate with a single powder layer; (c) powder layer with the laser path refined from 0% to 40%; (d) powder layer with the laser path refined from 20% to 60%; (e) powder layer with the laser path refined from 40% to 80%; (f) powder layer with the laser path refined from 60% to 100%; (g) substrate with two powder layers.

Table 1 presents the total number of finite elements used for each of the previous non-conformed meshes and compares it to the equivalent conformed mesh. For an conform mesh with elements equal in size to a level 3 element, a saving of about 49% is achieved with the non-conformed mesh. For an conform mesh with elements equal in size to a level 5 element, a saving of about 99% is achieved with the non-conformed mesh.

Table 1. Comparison of the number of FE needed with non-conform mesh and with conform mesh.

Mesh	Total number of elements	Comparison with conformal mesh equivalent to a uniform mesh of level 3 elements	Comparison with conformal mesh equivalent to a uniform mesh of level 5 elements
(a)	100	0.20%	0.00%
(b)	4650	9.08%	0.14%
(c)	26154	51.08%	0.80%
(d)	25993	50.77%	0.80%
(e)	26252	51.27%	0.80%
(f)	26252	51.27%	0.80%
(g)	8325	16.26%	0.25%

CONCLUSIONS

Since the finite element analysis of additive manufacturing processes is very time-consuming, this paper presents an algorithm to generate 3D non-conforming meshes, which are adapted for the specific features of these processes. The proposed adaptive mesh refinement uses an octree-based hierarchical data structure to improve the efficiency. The 2:1 balance constraint is imposed to reduce the number hanging nodes in the final mesh. Since the region around the laser beam contains the higher gradients in the state variables, the element size must be reduced in this region. However, during the process this region moves according to the laser path and velocity, which dictates the use of a dynamic adaptive mesh refinement/coarsening strategy. The shape of the moving heat source is adopted in the proposed algorithm to define the volume to be refined/coarsened. The powder laser deposition is modelled by refining the finite element mesh of newly activated elements until obtaining an element size identical to the thickness of the deposited powder layer. The initial conforming mesh (hexahedral elements) is iteratively modified through the refinement and coarsening procedures in order to reduce the total number of elements, without reducing the accuracy of the numerical solution. The results show that the proposed procedure enables the generation of non-conformal meshes with a total number of elements 99% lower than a conformal mesh with similar minimum element size.

ACKNOWLEDGMENTS

This research work was sponsored by national funds from the Portuguese Foundation for Science and Technology (FCT) under the project with reference PTDC/EME-EME/31657/2017 and by European Regional Development Fund (ERDF) through the Portugal 2020 program and the Centro 2020 Regional Operational Programme (CENTRO-01-0145-FEDER-031657) under the project MATIS (CENTRO-01-0145-FEDER-000014) and UID/EMS/00285/2020.

REFERENCES

[1] Khairallah, S.A., Anderson, A.T., Rubenchik, A., King, W.E., Laser powder-bed fusion additive manufacturing: Physics of complex melt flow and formation mechanisms of pores, spatter, and denudation zones. Acta Mater. 2016, 108, 36–45.

[2] Mercelis, P., Kruth, J.P., Residual stresses in selective laser sintering and selective laser melting. Rapid Prototyp. J. 2006, 12, 254–265.

[3] Papadakis, L., Loizou, A., Risse, J., Schrage, J., Numerical computation of component shape distortion manufactured by Selective Laser Melting, in: Procedia CIRP, Elsevier B.V., 2014, pp. 90–95.

[4] Leuders, S., Thöne, M., Riemer, A., Niendorf, T., et al., On the mechanical behaviour of titanium alloy TiAl6V4 manufactured by selective laser melting: Fatigue resistance and crack growth performance. Int. J. Fatigue 2013, 48, 300–307.

[5] Khairallah, S.A., Anderson, A., Mesoscopic simulation model of selective laser melting of stainless steel powder. J. Mater. Process. Technol. 2014, 214, 2627–2636.

[6] Gibson, I., Rosen, D., Stucker, B., Additive manufacturing technologies: 3D printing, rapid prototyping, and direct digital manufacturing, second edition, 2015.

[7] Eiser, S., Kaltenbacher, M., Nelhiebel, M., Non-conforming meshes in multi-scale thermo-mechanical Finite Element Analysis of semiconductor power devices, in: 2013 14th International Conference on Thermal, Mechanical and Multi-Physics Simulation and Experiments in Microelectronics and Microsystems, EuroSimE 2013, 2013.

[8] Riedlbauer, D., Steinmann, P., Mergheim, J., Thermomechanical finite element simulations of selective electron beam melting processes: Performance considerations. Comput. Mech. 2014, 54, 109–122.

[9] Berger, M.J., Oliger, J., Adaptive mesh refinement for hyperbolic partial differential equations. J. Comput. Phys. 1984, 53, 484–512.

[10] Olshanskii, M.A., Terekhov, K.M., Vassilevski, Y. V., An octree-based solver for the incompressible Navier-Stokes equations with enhanced stability and low dissipation. Comput. Fluids 2013, 84, 231–246.

[11] DebRoy, T., Wei, H.L., Zuback, J.S., Mukherjee, T., et al., Additive manufacturing of metallic components – Process, structure and properties. Prog. Mater. Sci. 2018, 92, 112–224.

[12] Samet, H., An Overview of Quadtrees, Octrees, and Related Hierarchical Data Structures, in: Theoretical Foundations of Computer Graphics and CAD, Springer Berlin Heidelberg, 1988, pp. 51–68.

[13] Sundar, H., Sampath, R.S., Biros, G., Bottom-up construction and 2:1 balance refinement of linear octrees in parallel. SIAM J. Sci. Comput. 2007, 30, 2675–2708.

[14] Goldak, J., Chakravarti, A., Bibby, M., A new finite element model for welding heat sources. Metall. Trans. B 1984, 15, 299–305.